Scientific Research Publishing

Fermi Energy-Incorporated Generalized BCS Equations for the Temperature-Dependent Critical Current Density and the Related Parameters of a Superconductor for All $T \leq T_c$ and Their Application to Aluminium Strips

Gulshan Prakash Malik[1*], Vijaya Shankar Varma[2#]

[1]B-208 Sushant Lok 1, Gurgaon, Haryana, India
[2]180 Mall Apartments, Mall Road, Delhi, India
Email: gulshanpmalik@yahoo.com, varma2@gmail.com

Abstract

Presented here are the Generalized BCS Equations incorporating Fermi Energy for the study of the {Δ, T_c, $j_c(T)$} values of both elemental and composite superconductors (SCs) for all $T \leq T_c$, where Δ, T_c and $j_c(T)$ denote, respectively, one of the gap values, the critical temperature and the T-dependent critical current density. This framework, which extends our earlier study that dealt with the {Δ_0, T_c, $j_c(0)$} values of an SC, is also shown to lead to T-dependent values of several other related parameters such as the effective mass of electrons, their number density, critical velocity, Fermi velocity (V_F), coherence length and the London penetration depth. The extended framework is applied to the $j_c(T)$ data reported by Romijn *et al.* for superconducting Aluminium strips and is shown not only to provide an alternative to the explanation given by them, but also to some novel features such as the role of the Sommerfeld coefficient $\gamma(T)$ in the context of $j_c(T)$ and the role of $V_F(T)$ in the context of a recent finding by Plumb *et al.* about the superconductivity of Bi-2212.

Keywords

$j_c(T)$ Data for Superconducting Aluminium Strips, Bardeen's Equation and Kupriyanov-Lukichev Theory for $j_c(T)$, Unified Generalized BCS Equations for {Δ, T_c, $j_c(T)$}, T-Dependence of the Sommerfeld Coefficient and Several Other Superconducting Parameters

*Formerly of the School of Environmental Sciences, Jawaharlal Nehru University, New Delhi, India.
#Formerly of the Department of Physics and Astrophysics, University of Delhi, Delhi, India.

1. Introduction

Adopting the framework of the Fermi energy (E_F)-incorporated generalized BCS equations (GBCSEs), we deal here with the calculation of the critical current density $j_c(T)$—for all T between 0 and T_c—of a superconductor (SC) which is not subjected to any external magnetic field. Specifically, we address here the data obtained by Romijn *et al.* [1] for superconducting aluminium strips for which it suffices to apply GBCSEs in the scenario where Cooper pairs (CPs) are formed via the one-phonon exchange mechanism (1 PEM). However, with high-T_c SCs in mind, also given here are GBCSEs that enable one to deal in a unified manner with the gaps (Δs), T_c and $j_c(T)$ of a composite, multi-gapped SC requiring more than 1 PEM.

The paper is organized as follows. In order to provide a perspective of the conceptual basis of the conventional, multi-band approach (MBA) to the study of the set {Δ, T_c, $j_c(T)$} of a composite SC vis-à-vis that of the GBCSEs-based approach, we include in this section an overview of both approaches. Since the data in [1] are explicable in the conventional approach via both the phenomenological Bardeen equation [2] and the Kupriyanov and Lukichev (KL) [3] theory discussed below, the purpose of this paper is to show that the GBCSEs-based approach provides a valuable alternative explanation of the same data. In the next section are given the E_F-incorporated GBCSEs in the scenario when a two-phonon exchange mechanism (2 PEM) is operative. These equations provide a unified framework for the description of the set {Δ_2, T_c, j_0}, where Δ_2 is the larger of the two gaps of the SC. Application of the GBCSEs to the $j_c(T)$ data in [1] is taken up in Section 3 where they are also shown to provide the values of several other related T-dependent parameters such as the Sommerfeld coefficient, the effective mass of electrons, their number density, critical velocity, Fermi velocity, coherence length and the London penetration depth. Sections 4 and 5 are devoted, respectively, to a Discussion of our approach and the Conclusions following from it.

1.1. Overview of the Conventional Approach in Dealing with the Set {Δ, T_c, $j_c(T)$} of a Composite SC

The gaps of a hetero-structured SCs are most widely studied via an adaptation of the multi-band approach (MBA) of Suhl *et al.* [4]. When such a study also deals with a T_c of the SC, which is not always the case, it generally appeals to the Migdal-Eliashberg-McMillan approach (MEMA) [5]. Even though MEMA is cast in the BCS mould of a 1-phonon exchange mechanism (1 PEM) for the formation of CPs, it is employed to deal with such high-T_cs as are observed because it permits the BCS interaction parameter λ to even exceed unity because it is based on an integral equation the expansion parameter of which is not λ, but m_e/M where m_e is the electron mass and M the mass of an ion. Insofar as j_c is concerned, a plethora of formulae is conventionally employed depending upon the type of the SC (I or II), its size, shape and the manner of preparation—for some such formulae which do not take into account the T-dependence of j_c, see [6].

Insofar as $j_c(T)$ is concerned, it is empirically known that it has its maximum value at $T = 0$ and that $j_c(T_c) = 0$. It took considerable time for theoretical attempts to evolve before the observed variation of $j_c(T)$ between these limits could be explained. Perhaps the earliest such attempt was due to London, who gave an equation for $j_c(T)$ valid at $T = T_c$, but which failed at lower temperatures because, as was later realized, it did not take into account the effect of the change in the order parameter with current/temperature. The equation for $j_c(T)$ given by the phenomenological Ginzberg-Landau (GL) theory marks the next stage in the said evolution. This equation works well close to T_c, but not for much lower temperatures. As is well known, the GL theory reduces to the London theory when the concentration of superconducting electrons is uniformly distributed and that, as was shown by Gor'kov, the microscopic theory in which the energy gap is taken as an order parameter leads to the GL theory near T_c. These brief considerations suggest the need to appeal to the microscopic theory in order to explain the observed variation of $j_c(T)$ for all $T \leq T_c$. Before we do so, it is relevant to draw attention to a phenomenological equation for $j_c(T)$ given by Bardeen [2] post-BCS. This equation, valid for all T between 0 and T_c and obtained by treating the gap as a variational parameter and minimizing the free energy for a given current, is

$$j_c(T) = \frac{1}{2\sqrt{2}} j_c(0) \left[1 - (T/T_c)^2 \right]^{3/2}. \tag{1}$$

Equation (1) is applicable to SCs for which changes in the energy gap with position can be neglected.

Since the thin samples of Romijn *et al.* [1] satisfied the condition(s) of validity of (1), they applied it to one of their samples and found that it indeed fits their data well. Nonetheless, (1) does not address the core issue of the problem, *i.e.*, to identify the parameters on which $j_c(T)$ depends. The knowledge of these is essential because it provides a handle to control $j_c(T)$. To unravel what lies beneath the "blanket" of (1), one needs a microscopic theory, viz. the theory given by Eilenberger which is derived from the original Gor'kov theory under the assumption $\rho_F \ell \gg 1$, where ρ_F is the electrical resistivity of electrons at the Fermi surface and ℓ their mean free path. It was shown by KL [3] that for an SC subject to certain constraints, the Eilenberger equations can be further simplified. Since their samples satisfied these conditions, Romijn *et al.* [1] also employed approximate solutions of the KL equations and found that their data were thus adequately explained.

1.2. Overview of the GBCSEs-Based Approach in Dealing with the Set {Δ, T_c, $j_c(T)$} of a Composite SC

Complementing MBA and presented in a recent monograph [7] is an approach based on the GBCSEs which too has been applied to a significant number of SCs. One of the premises of this approach is that Fermi energy (E_F) plays a fundamental role in determining the superconducting properties of an SC. We recall

in this connection that the usual BCS equations for the T_c and Δ of an elemental SC are independent of E_F because of the assumption that $E_F \gg k\theta$, where k is the Boltzmann constant and θ the Debye temperature of the SC. GBCSEs are obtained via the Matsubara technique and a Bethe-Salpeter equation (BSE) the kernel of which is a super propagator. The latter feature leads to the characterization of a composite SC by CPs with multiple binding energies ($|W|$s). A salient feature of this approach is that it invariably invokes a λ for each of the ion-species that may cause pairing, whence one has the same λs in the equations for any Δ and the corresponding T_c of the SC—as is the case for elemental SCs. Multiple gaps arise in this approach because different combinations of λs operate on different parts of the Fermi surface due to its undulations. Each of the $|W|$s so obtained is identified with a Δ of the SC. Thus, as shown in [7], with the input of the values of any two gaps of an SC and a value of its T_c, this approach goes on to shed light on several other values of these parameters. This is not so for MBA, another feature of which is that even when it is employed to deal with the same SC by different authors, the number of bands invoked is not always the same.

2. E_F-Incorporated GBCSEs for the T_c, Δs and j_c of a Hetero-Structured SC

2.1. Equations for $|W_{20}|$ (To Be Identified with Δ_{20}, the Larger of the Two Gaps at $T = 0$), $W_2(t = T/T_c)$ and T_c [7]

The equation for $|W_{20}|$ is:

$$\frac{\lambda_1}{2} a_1\left(\theta_1, \mu, W_{20}\right) + \frac{\lambda_2}{2} a_2\left(\theta_2, \mu, W_{20}\right) = \left[\frac{3}{4} a_3\left(\mu, W_{20}\right)\right]^{1/3}, \tag{2}$$

where

$$a_1\left(\theta_1, \mu, W_{20}\right) = \boldsymbol{Re}\left[\int_{-k\theta_1}^{k\theta_1} \mathrm{d}\xi \frac{\sqrt{\xi + \mu}}{|\xi| + |W_{20}|/2}\right], \quad a_2\left(\theta_2, \mu, W_{20}\right) = a_1\left(\theta_2, \mu, W_{20}\right)$$

$$a_3\left(\theta_m, \mu, W_{20}\right) = \boldsymbol{Re}\left[\frac{4}{3}\left(\mu - k\theta_m\right)^{3/2} + \int_{-k\theta_m}^{k\theta_m} \mathrm{d}\xi \sqrt{\xi + \mu}\left(1 - \frac{\xi}{\sqrt{\xi^2 + W_{20}^2}}\right)\right]. \tag{3}$$

The equation for $|W_2(t)|$ for $0 < t < 1$ is:

$$\lambda_1 b_1\left(\theta_1, \mu, W_2\right) + \lambda_2 b_2\left(\theta_2, \mu, W_2\right) = \left[\frac{3}{4} b_3\left(\theta_m, \mu, W_2\right)\right]^{1/3}, \tag{4}$$

where

$$b_1\left(\theta_1, \mu, W_2\right) = b_{11}\left(\theta_1, \mu, W_2\right) + b_{12}\left(\theta_1, \mu, W_2\right)$$

$$b_2\left(\theta_2, \mu, W_2\right) = b_{21}\left(\theta_2, \mu, W_2\right) + b_{22}\left(\theta_2, \mu, W_2\right)$$

$$b_{11}\left(\theta_1, \mu, W_2\right) = \int_{-k\theta_1}^{0} \mathrm{d}\xi \sqrt{\mu + \xi} \frac{\tanh\left[\left(1/2\,ktT_c\right)\left(\xi - W_2\right)\right]}{\xi - W_2}$$

$$b_{12}\left(\theta_1, \mu, W_2\right) = \int_{0}^{k\theta_1} \mathrm{d}\xi \sqrt{\mu + \xi} \frac{\tanh\left[\left(1/2\,ktT_c\right)\left(\xi + W_2\right)\right]}{\xi + W_2}$$

$$b_{21}(\theta_2, \mu, W_2), \ b_{22}(\theta_2, \mu, W_2) = b_{11}(\theta_2, \mu, W_2), \ b_{12}(\theta_2, \mu, W_2)$$

$$b_3(\theta_m, \mu, W_2) = \int_{-\mu}^{k\theta_m} \sqrt{\mu + \xi} \left[1 - \frac{\xi \tanh\left[(1/2\,ktT_c)\sqrt{\xi^2 + W_2^2} \right]}{\sqrt{\xi^2 + W_2^2}} \right],$$

and the equation for T_c is:

$$\frac{\lambda_1}{2} c_1(\theta_1, \mu, T_c) + \frac{\lambda_2}{2} c_2(\theta_2, \mu, T_c) = \left[\frac{3}{4} c_3(\theta_m, \mu, T_c) \right]^{1/3}, \qquad (5)$$

where

$$c_1(\theta_1, \mu, T_c) = \boldsymbol{Re}\left[\int_{-\theta_1/2T_c}^{\theta_1/2T_c} \mathrm{d}x \sqrt{2kT_c x + \mu} \, \frac{\tanh(x)}{x} \right]$$

$$c_2(\theta_2, \mu, T_c) = c_1(\theta_2, \mu, T_c)$$

$$c_3(\theta_m, \mu, T_c) = \boldsymbol{Re}\left[2kT_c \int_{-\theta_m/2T_c}^{\theta_m/2T_c} \mathrm{d}x \sqrt{2kT_c x + \mu} \left\{ 1 - \tanh(x) \right\} \right]$$

In the above equations, θ_1 and θ_2 are the Debye temperatures of the ion-species that cause pairing and are obtained from the Debye temperature θ of the SC as detailed in [7] and [8]; θ_m is the greater of the temperatures θ_1 and θ_2, and the variation of chemical potential with temperature has been ignored in order to avoid the situation where we have an under-determined set of equations. Thus, we have assumed that the chemical potential $\mu(T=0) = \mu(T=T_c) = E_F$. With the input of $|W_{20}|$, T_c, and different assumed values of $\mu = \rho k\theta$ ($\rho = 100, 50, 25, 10, 5$, etc.), solution of simultaneous Equations (2) and (4) yields, for each value of μ, the corresponding values of the interaction parameters λ_1 and λ_2.

2.2. Equation for a Dimensionless Construct y_0 at $T = 0$ Which Enables One to Calculate j_0 and Several Other Superconducting Parameters

The construct y_0 is defined as

$$y_0 = (k\theta/P_0)\sqrt{2m^*(0)/E_F}, \qquad (6)$$

where $m^*(0)$ is the effective mass of superconducting electrons at $T = 0$ and P_0 their critical momentum.

The exercise carried out above leads to a multitude of values for the set $S = \{E_F, \lambda_1, \lambda_2\}$, each of which is consistent with the $|W_{20}|$ and T_c values of the SC. In order to find the unique set of values from among them that also leads to the empirical value of j_0 of the SC, we solve the following equation for y_0 [9] for each triplet of $\{E_F, \lambda_1, \lambda_2\}$ values:

$$1 = \frac{\lambda_1}{4} J(\Sigma_1', r_1 y_0) + \frac{\lambda_2}{4} J(\Sigma_2', r_2 y_0), \qquad (7)$$

where

$$J(\Sigma', y_0) = \boldsymbol{Re}\left[\int_0^1 \mathrm{d}x F(\Sigma', x, y_0) \right], \quad F(\Sigma', x, y_0) = f_1(\Sigma', x, y_0) + f_2(\Sigma', x, y_0)$$

$$f_1(\Sigma', x, y_0) = 4\left[-u_1(\Sigma', x, y_0) - u_2(\Sigma', x, y_0) + u_3(\Sigma', x, y_0) + u_4(\Sigma', x, y_0) \right]$$

$$f_2\left(\Sigma', x, y_0\right)$$

$$= 2\ln\left[\frac{1+u_1\left(\Sigma', x, y_0\right)}{1-u_1\left(\Sigma', x, y_0\right)}\frac{1+u_2\left(\Sigma', x, y_0\right)}{1-u_1\left(\Sigma', x, y_0\right)}\frac{1-u_3\left(\Sigma', x, y_0\right)}{1+u_3\left(\Sigma', x, y_0\right)}\frac{1-u_4\left(\Sigma', x, y_0\right)}{1+u_4\left(\Sigma', x, y_0\right)}\right]$$

$$u_1\left(\Sigma', x, y_0\right) = \sqrt{1-\Sigma' x/y_0}, \quad u_2\left(\Sigma', x, y_0\right) = \sqrt{1+\Sigma' x/y_0}$$

$$u_3\left(\Sigma', x, y_0\right) = \sqrt{1-\Sigma'\left(1-x/y_0\right)}, \quad u_4\left(\Sigma', x, y_0\right) = \sqrt{1+\Sigma'\left(1-x/y_0\right)}$$

$$\Sigma' = k\theta/E_F, \quad \Sigma'_i = k\theta_i/E_F, \quad r_i = \theta_i/\theta.$$

The operator **Re** ensures that the integrals yield real values even when expressions under the radical signs are negative (as happens for the heavy fermion SCs).

Corresponding to *each* value of y_0 obtained by solving (6) with the input of $\{\theta, \theta_1, \theta_2, E_F, \lambda_1, \lambda_2\}$, we can calculate several superconducting parameters in terms of θ, E_F, y_0, the gram-atomic volume v_g and the electronic heat constant/Sommerfeld coefficient γ_0 at $T = 0$ by employing the following relations, see [8] and for a correction, [10]:

$$s(0) \equiv m^*(0)/m_e = A_1\frac{\left(\gamma_0/v_g\right)^{2/3}}{E_F^{1/3}} \tag{8}$$

$$N_{s0}\left(E_F\right) = A_2\left(\gamma_0/v_g\right)E_F \tag{9}$$

$$P_0\left(E_F\right) = A_3\frac{\theta}{y_0}\frac{\left(\gamma_0/v_g\right)^{1/3}}{E_F^{2/3}} \tag{10}$$

$$V_{c0}\left(E_F\right) = A_4\frac{\theta}{y_0}\frac{1}{\left(\gamma_0/v_g\right)^{1/3}E_F^{1/3}} \tag{11}$$

$$j_0\left(E_F\right) = \frac{N_{s0}\left(E_F\right)}{2}e^*V_{c0}\left(E_F\right) = A_5\frac{\theta}{y_0}\left(\gamma_0/v_g\right)^{2/3}E_F^{2/3}, \quad \left(e^* = 2e\right) \tag{12}$$

where m_e is the free electron mass and e the electronic charge,

$$A_1 \cong 3.305\times10^{-10}\ \text{eV}^{-1/3}\cdot\text{cm}^2\cdot\text{K}^{4/3}, \quad A_2 \cong 2.729\times10^7\ \text{eV}^{-2}\cdot\text{K}^2,$$

$$A_3 \cong 1.584\times10^{-6}\ \text{cm}\cdot\text{K}^{-1/3}, \quad A_4 \cong 1.406\times10^8\ \text{eV}^{2/3}\cdot\text{sec}^{-1}\cdot\text{K}^{-5/3},$$

$$A_5 \cong 6.146\times10^{-4}\ \text{C}\cdot\text{eV}^{-4/3}\cdot\text{K}^{1/3}\cdot\text{s}^{-1},$$

and N_{s0} is the number density of CPs and V_{c0} their critical velocity at $T = 0$. Comparison of the j_0-values so obtained with the experimental value of j_0 then leads to the desired unique set of $\{E_F, \lambda_1, \lambda_2\}$-values that is consistent with the empirical values of $|W_{20}|$, T_c, and j_0 of the SC.

2.3. Equation for the Dimensionless Construct $y(t) = \left(k\theta/P_c(t)\right)\sqrt{2m^*/E_F(t)}$ Which Enables One to Calculate $j_c(t)$ and Several Other Superconducting Parameters at $t \neq 0$

When $t \neq 0$, the equation for $y(t)$ is obtained from [9]

$$1 = \frac{\lambda_1}{4} \int_0^1 dx \left[I_1(x, \theta_1, E_2) + I_2(x, \theta_1, E_2) \right]$$
$$+ \frac{\lambda_2}{4} \int_0^1 dx \left[I_1(x, \theta_2, E_2) + I_2(x, \theta_2, E_2) \right], \tag{13}$$

where

$$I_1(x, \theta, E_2) = \int_{-E_1 + E_2 x}^{E_1 - E_2 x} d\xi \, \phi(\xi) \tanh \left[(\beta/2)(\xi + E_2 x) \right]$$

$$I_2(x, \theta, E_2) = \int_{-E_1 + E_2 x}^{E_1 - E_2 x} d\xi \, \phi(\xi) \tanh \left[(\beta/2)(\xi - E_2 x) \right]$$

$$\phi(\xi) = \sqrt{1 + \xi/E_F} / (\xi + E_3), \quad E_1 = k\theta$$

$$E_2(t) = P_c(t) \sqrt{E_F/2m^*(t)}, \quad E_3(t) = P_c^2(t)/8m^*(t), \quad \beta = 1/ktT_c.$$

In terms of $y(t) = E_1/E_2(t) = \left[k\theta/P_c(t) \right] \sqrt{2m^*(t)/E_F}$, we have (12) as:

$$1 = \frac{\lambda_1}{4} \int_0^1 dx f(x, \theta_1, E_F, r_1 y) + \frac{\lambda_2}{4} \int_0^1 dx f(x, \theta_2, E_F, r_2 y), \tag{14}$$

where

$$f(x, \theta, E_F, y)$$
$$= \int_{-E_1(1-x/y)}^{E_1(1-x/y)} d\xi \, \phi(\xi, E_F, y) \left\{ \tanh \left[\frac{\theta}{2tT_c y} \left(\frac{\xi y}{k\theta} + x \right) \right] + \tanh \left[\frac{\theta}{2tT_c y} \left(\frac{\xi y}{k\theta} - x \right) \right] \right\}$$

$$E_1 = k\theta, \quad \phi(\xi, E_F, y) = \sqrt{1 + \xi/E_F} / \left[\xi + E_3(y) \right],$$

$$E_3(y) = E_1^2 / 8m^* \alpha^2 y^2, \quad r_i = \theta_i / \theta.$$

Each value of $y(t)$ obtained by solving (13) for different values of the set $S = \{E_F, \lambda_1, \lambda_2\}$ leads to the corresponding value of $j_c(t)$ via (11), and to the values of the associated parameters via (7)-(10).

3. Explanation of the Empirical $j_c(t)$ Values of Aluminium Strips Via GBCSEs

By adding to the RHS of each of the Equations (2), (3), and (4) a term in which λ_2 and θ_2 are replaced by λ_3 and θ_3, respectively, the above framework is easily extended to a 3PEM scenario where pairing is caused by three ion-species. On the other hand, in order to deal with the data reported for Aluminium strips in [1], we need the reduced framework of 1 PEM. This is obtained by putting $\lambda_2 = 0$ in each of the three equations just noted.

3.1. The j_0 Data

Reported in [1] are various superconducting properties for six samples of aluminium strips at $T = 0$. Among these, T_c and j_0 are determined experimentally, whereas values of some other parameters such as coherence length ξ and the London penetration depth λ_L are model-dependent derived properties.

In order to show how the GBCSEs-based approach works in such a situation, we give below the sequential steps that are followed for Sample 1 in [1].

1) The T_c of the sample is 1.196 K. We take its Debye temperature θ to be 428 K [11]. Employing these values and putting $\lambda_2 = 0$ (as is appropriate for a 1 PEM), solution of (4) for some typical values of E_F are: $\lambda_1 = 0.1665$ for any value of $E_F = 10$ - $100k\theta$; $\lambda_1 = 0.1666$ for $E_F = 5k\theta$, $\lambda_1 = 0.1670$ for $E_F = 2k\theta$.

2) For some select pairs of $\{E_F, \lambda_1\}$ values obtained above, we now solve (6) for the corresponding value of y_0 and obtain the following results (in the parentheses are given the $\{E_F, \lambda_1\}$ values): $y_0 = 149.8$ $\{50k\theta, 0.1665\}$; $y_0 = 149.9$ $\{25k\theta, 0.1665\}$; $y_0 = 149.9$ $\{10k\theta, 0.1665\}$; $y_0 = 149.6$ $\{5k\theta, 0.1666\}$; $y_0 = 149.5$ $\{2k\theta, 0.1670\}$.

3) For each of the above pairs of $\{E_F, y_0\}$ values, we now calculate j_0 via (11). For this purpose, besides the value of θ, we require the values of γ_0 and v_g which are taken as: $\gamma_0 = 1.36$ mJ/mol-K^2 [11], $v_g = 10$ cm^3/gram-atom. The results in A/cm^2 with the corresponding $\{E_F, y_0\}$ values given in parentheses are: 2.37×10^7 $\{50k\theta, 149.8\}$, 1.49×10^7 $\{25k\theta, 149.8\}$ 8.09×10^6 $\{10k\theta, 149.9\}$, 5.11×10^6 $\{5k\theta, 149.6\}$, 2.77×10^6 $\{2k\theta, 149.5\}$.

4) Among the above values, $j_0 = 1.49 \times 10^7$ A/cm^2 corresponding to $\{E_F = 25k\theta, y_0 = 149.8\}$ is closest to the experimental value of 1.53×10^7 A/cm^2. By fine-tuning the value of E_F and repeating the above exercise, we find that the experimental value of j_0 is obtained exactly when $E_F = 26k\theta = 0.959$ eV and $y_0 = 149.8$.

5) With E_F fixed at this value, we can find W_{10} via (2) (with $\lambda_2 = 0$).

6) With E_F and y_0 of the sample fixed as above, we can calculate the values of $s(0)$, $N_s(0)$, and V_{c0} via (7), (8) and (10), respectively, and the Fermi velocity V_{F0} at $T = 0$ via the relation

$$(1/2)m^*(0)V_{F0}^2 = E_F. \tag{15}$$

Besides these parameters, we can now also calculate the coherence length ξ_0 at $T = 0$ via

$$\xi_0 = \hbar V_{F0}/\pi|W_{10}|, \tag{16}$$

and the London penetration depth λ_{L0} at $T = 0$ via

$$\lambda_{L0} = \sqrt{m^*(0)cm^3(\hbar c)^2/4\pi n_s(0)e^2}, \tag{17}$$

where units for m^* and n_s are electron-volt and cm^{-3}, respectively, $e = (137.03604)^{-1/2}$, $cm = 5.067728861 \times 10^4(\hbar c)$ eV^{-1} and, for convenience of the reader, we have inserted the requisite factors of $\hbar$ and c in order to obtain the value of λ_{L0} in cgs units. The results of these calculations are given in Table 1, which also gives similar results for the remaining five samples dealt with in [1].

3.2. The $j_c(t)$ Data

Insofar as $j_c(t)$ is concerned, Romijn et al. [1] have given results for one of their samples (Sample 5) in their Figure 4, which is a plot of their experimental values of $\left[j_c(t)/j_c(0)\right]^{2/3}$ along with their counterparts as obtained via the phenomenological Bardeen Equation (1) and the KL theory [3]. It follows from this

Table 1. For the samples employed in [1], the $T = 0$ values of various superconducting parameters obtained via the procedure detailed in Section 3.1.

Sample	T_c (K)	j_0 (exp) (10^7 A/cm^2)	j_0 (theory) (10^7 A/cm^2)	ρ ($E_F = \rho k\theta$)	λ_1	y_0	s	$N_s(0)$ (10^{22} cm^{-3})	V_0 (10^3 cms^{-1})	V_F (10^7 cms^{-1})	$|W_1|$ (10^{-4} eV)	ξ_0 (10^{-5} cm)	λ_{L0} (10^{-6} cm)
1	1.196	1.53	1.53	26	0.1665	149.8	3.005	2.22	4.30	3.35	1.82	3.88	6.18
2	1.203	1.30	1.29	20	0.1667	148.8	3.279	1.71	4.73	2.81	1.84	3.26	7.36
3	1.203	1.56	1.58	27	0.1667	148.7	2.967	2.31	4.28	3.44	1.84	3.98	6.03
4	1.267	1.11	1.12	15	0.1681	141.6	3.609	1.28	5.47	2.32	1.93	2.98	8.92
5	1.356	1.07	1.07	12.6	0.1701	132.0	3.825	1.07	6.21	2.07	2.07	2.39	10.0
6	1.154	2.57	2.55	59	0.1655	155.3	2.287	5.04	3.36	5.79	1.82	6.70	3.58

graph that the absolute experimental values of $j_c(t)$ are given fairly accurately by

$$j_c(t)\big|_{\exp} \simeq j_0\big|_{\exp}\left(1 - t^2\right)^{3/2},\tag{18}$$

where $j_0\big|_{\exp} = 1.07 \times 10^7 \text{ A/cm}^2$.

We recall that j_0 of Sample 5 in our approach was calculated via the following values of the associated parameters: $\theta = 428$ K, $T_c = 1.356$ K, $\lambda_1 = 0.1701$, $E_F = 12.6k\theta$, $y_0 = 132.0$, $\gamma_0 = 1.36$ mJ/mol K^{-2}, and $v_g = 10$ cm^3/gram-atom. In order now to calculate $j_c(t)$ for this sample, we need to take into account the T-dependence of all these parameters. It seems reasonable to assume that among them, θ, E_F and v_g retain the values employed for them at $T = 0$. This assumption enables us to calculate $y(t)$ for any "t" via (13) (with $\lambda_2 = 0$); the resulting values are given in **Table 2**. We could now calculate $j_c(t)$ if we knew $\gamma(t)$, but about which we have no information. However, we know that the heat capacity of an SC has a marked non-linear dependence on t as discussed, e.g. in general in [12] and for superconducting Ga in ([13], p. 411). We are hence led to calculate $\gamma(t)$ with the input of $j_c(t)$—rather than the other way around—via the following equation

$$j_c(t)\big|_{\exp} = j_c\left(\theta, y(t), \gamma(t), v_g, E_F\right)\big|_{\text{Th}},\tag{19}$$

the LHS of which for any "t" is taken to be given by (17) and the RHS is calculated via (11) with the input of $y(t)$ obtained by solving (13). These values of $\gamma(T)$ are included in **Table 2**. Considered together with the values of $y(t)$, they will be shown below to provide a microscopic justification of Bardeen's phenomenological Equation (1). It is also remarkable that $y(t)$ and $\gamma(t)$ enable one to obtain quantitative estimates of several other t-dependent superconducting parameters, viz., $s(t) = m^*(t)/m_e$, $n_s(t) = N_s(t)/N_{s0}$, $v_F(t) = V_F(t)/V_{F0}$, $v_c(t) = V_c(t)/V_0$, $\xi_r(t) = \xi(t)/\xi_0$, and $\lambda_{Lr}(t) = \lambda_L(t)/\lambda_{L0}$. The plots of these are discussed below.

4. Discussion

1) The T-dependence of $\gamma(T)$ in the context of $j_c(t)$ is a new feature of the approach followed here. We recall that, as is well known, γ is usually defined via the equation

Table 2. Obtained as detailed in Section 3.2, values of $y(t)$ and $\gamma(t)$ corresponding to the experimental values of $j_c(t)$ for Sample 5 in [1] for $0 \leq t \leq 1$.

t	$j_c(t)\big|_{\exp} \times 10^6 \, (\text{A}/\text{cm}^2)$	$y(t)$	$\gamma(t) \times 10^{-4} \, (\text{J}/\text{mol} \cdot \text{K}^{-2})$
0	10.7	132.0	13.6
0.1	10.5	132.4	13.3
0.2	10.1	133.6	12.6
0.3	9.29	133.9	11.5
0.4	8.24	139.9	10.0
0.5	6.95	145.9	8.25
0.6	5.48	155.9	6.38
0.7	3.90	172.6	4.46
0.8	2.31	203.2	2.60
0.9	0.89	276.8	0.99
0.95	0.33	384.5	0.36
1	0	-	-

$$C_p = C_v = \gamma T + 464.6\left(T/\theta\right)^3, \tag{20}$$

where C_p (C_v) is the heat capacity of the SC at constant pressure (volume) at very low temperatures (<10 K). The experimental data are usually plotted in the form C_v/T vs. T^2, which yields an intercept equal to γ and a slope equal to $464.6/\theta^3$. The generally reported values of γ in the literature, e.g. in [11], obtained in this manner correspond to $T = 0$. It should also be noted that the simple relation (19) is invalid when the magnetic and nuclear contributions may be significant and, importantly, that γ is directly proportional to $N(E_F)$, the density of states of electrons at the Fermi level. The latter of these features implies that we are taking into account the T-dependence of $N(E_F)$ via $\gamma(T)$.

2) It was assumed above that among the five parameters that are required for the calculation of $j_c(t)$ via (11), we need to take into account the T-dependence of only two of them, viz., y and γ. Since the T-dependence of $j_c(t)$ is then governed by $R(t) \equiv \left[\gamma(t)\right]^{2/3}/y(t)$, we give for Sample 5 in [1] a plot of $R(t)$ vs. t in **Figure 1**, where $\gamma(t)$ and $y(t)$ are obtained via solutions of (18) and (13), respectively. Included in this figure is a plot of the ratio $R_1(t) = \left[\gamma(0)^{2/3}/y(0)\right]\left(1-t^2\right)^{3/2}$ vs. t, which is seen to be almost indistinguishable from the plot of $R(t)$. It therefore follows that our approach based on the microscopic BSE provides a detailed theoretical justification of the phenomenological Bardeen Equation (1) for $j_c(t)$.

3) In the approach followed in [1], while both $j_c(0)$ and $j_c(t \neq 0)$ depend on e, T_c, V_F, ρ_F and ℓ, the expression for the latter requires additional parameters as is seen from the Appendix in [1]. In the approach followed in this paper, no such additional parameters are required to deal with $j_c(t \neq 0)$; one simply invokes, where applicable, the T-dependence of the parameters on which $j_c(0)$ depends, viz. e, θ, y_0, γ_0, v_g and E_F. The two approaches may therefore be said to complement each other.
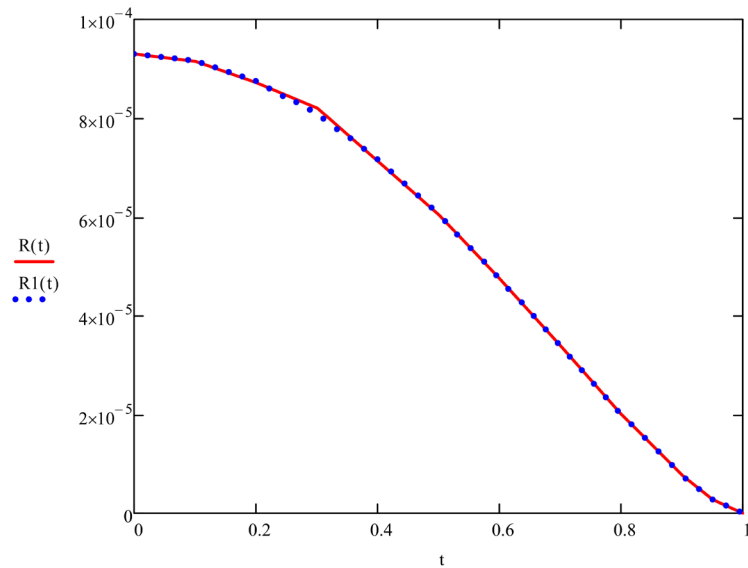
Figure 1. For Sample 5 in [1]: plots of $R(t) \equiv \left[\gamma(t)\right]^{2/3} \Big/ y(t)$ as obtained via solutions of (18) and (13), respectively, and of $R_1(t) = \left[\gamma(0)^{2/3} \Big/ y(0)\right]\left(1-t^2\right)^{3/2}$.

4) The expression for $j_c(0)$ in [1] depends on V_F, which is not so in the GBCSEs-based approach where $j_c(0)$ depends on $V_c(0)$. Nonetheless, it is interesting to note that the value of V_F in [1] is assumed to be 1.36×10^8 cm/s for all samples and is not T-dependent whereas, in the approach followed here, it differs from sample to sample and is T-dependent. For Sample 5, it varies between $(2.07 - 6.95) \times 10^7$ cm/sec for $0 \leq t \leq 1$. For this sample, the values of ξ_0 and λ_{L0} too differ in the two approaches: while reported in [1] for these parameters are, respectively, the values 1.32×10^{-4} cm and 1.10×10^{-4} cm, the corresponding values determined by us are 2.39×10^{-5} cm and 1.00×10^{-5} cm.

5) Given in **Figure 2** are the plots of $w_1(t)$, $s(t)$ and $n_s(t)$ vs. t for Sample 5 in [1]. Among these, even though the plot of $w_1(t)$ is obtained via an E_F-incorporated GBCSE with $E_F = 12.6k\theta$, it is very similar to the plot one obtains for $\Delta(T)/\Delta_0$ for an elemental SC via the usual BCS equation sans E_F. While we could not find any experimental data for the parameter $s(t) \equiv m^*(T)/m_e$ for the SC under consideration, we draw attention to a plot of this parameter for Pb and Ta given in (Figure 7 of [12]). This plot covers temperatures up to about 120 K and therefore does not specifically shed light on the behavior of $s(t)$ in the superconducting state. Nonetheless, it is notable that it displays a parabolic decrease for a major part of the range of temperatures over which it is plotted. As for $n_s(t)$, as shown in **Figure 2**, we find that a good analytic fit to the values calculated by us is provided by $n_s(t) = \left(1-t^2\right)^{1.51}$, which is at variance with the result of the simple two-fluid model where $n_s(t) = \left(1-t^4\right)$. However, it is also well known that, factually, T-dependences of superconducting parameters often differ from those following from the simple two-fluid model ([11], p. 48).

6) In the context of **Figure 3** which is the plot of the reduced fermi velocity v_F that our approach has led to, we draw attention to a paper by Plumb *et al.* [14]

who have reported that "Associated with this feature (a kink-like feature observed at extremely low energy along the superconducting node in Bi-2212), the Fermi velocity scales substantially—increasing by roughly 30% from 70 to 110 K. The temperature dependence of the feature suggests a possible role in superconductivity, although it is unclear at this time what mechanism(s) may lead to this low-energy renormalization". We are hence led to suggest that **Figure 3** provides both: a plausible explanation that Plumb *et al.* sought for their result and a validation of our approach.
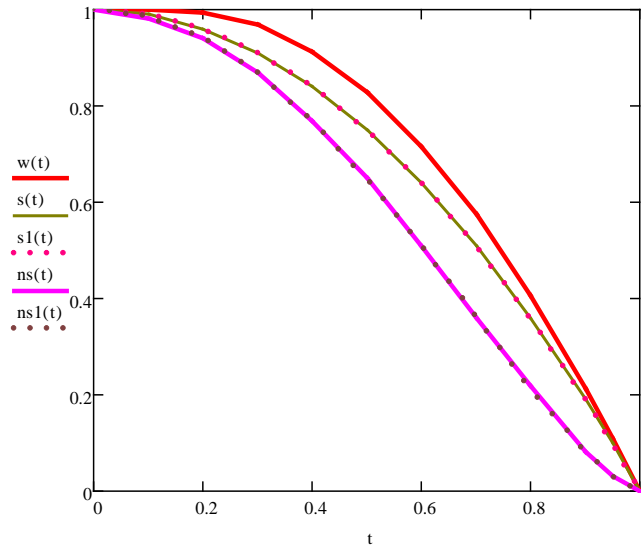
Figure 2. For Sample 5 in [1]: clockwise, solid lines represent $w(t) = W_1(T)/W_{10}$, $s(t) = m^*(T)/m_e$, and $n_s(t) = N_s(T)/N_{s0}$ calculated via, respectively, (3), and the T-generalized (7) and (8). For values of W_{10}, $s(0)$ and N_{s0}, see **Table 1**. The dotted plot overlapping $s(t)$ is the analytic fit to it obtained via $s_1(t) = (1 - t^2)$; the plot overlapping $n_s(t)$ is a similar plot obtained via $n_{s1}(t) = \left(1 - t^2\right)^{1.51}$.
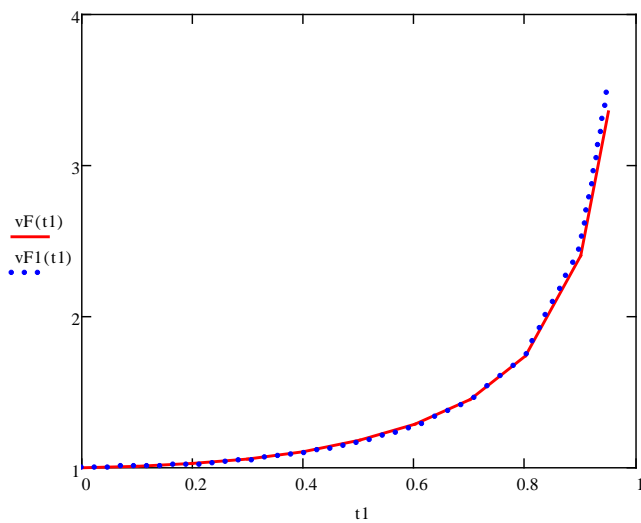

Figure 3. Plot of the reduced fermi velocity $v_F(t) = V_F(T)/V_{F0}$ corresponding to Sample 5 in [1]. The dotted plot overlapping it is obtained via $v_{F1}(t_1) = \left(1 - t_1^2\right)^{-0.54}$.

7) Both $\xi_r(t)$ and $\lambda_{Lr}(t)$ are known to diverge at $t = 1$, which is a feature also reflected in our **Figure 4** and **Figure 5**. It is thereby seen that for the former parameter, $\xi_1(t) = \left(1 - t_1^2\right)^{-1.41}$ provides a good fit to $\xi_r(t)$, whereas a similar fit for the latter parameter is provided by $\lambda_{L1}(t) = \left(1 - t^2\right)^{-0.27}$.
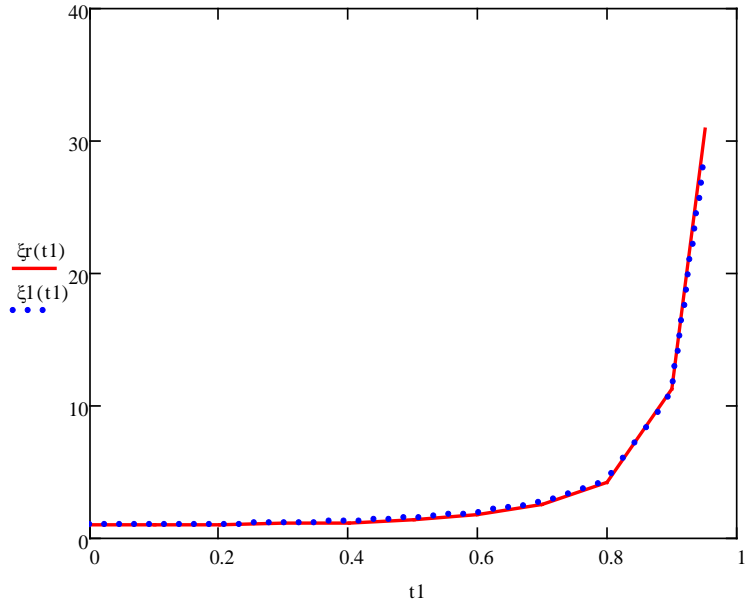

Figure 4. For Sample 5 in [1], the solid line is the plot of the reduced coherence length $\xi_r(t) = \xi(T)/\xi_0$ as obtained via theory in this paper. The overlapping plot is obtained via $\xi_1(t_1) = \left(1 - t_1^2\right)^{-1.41}$.
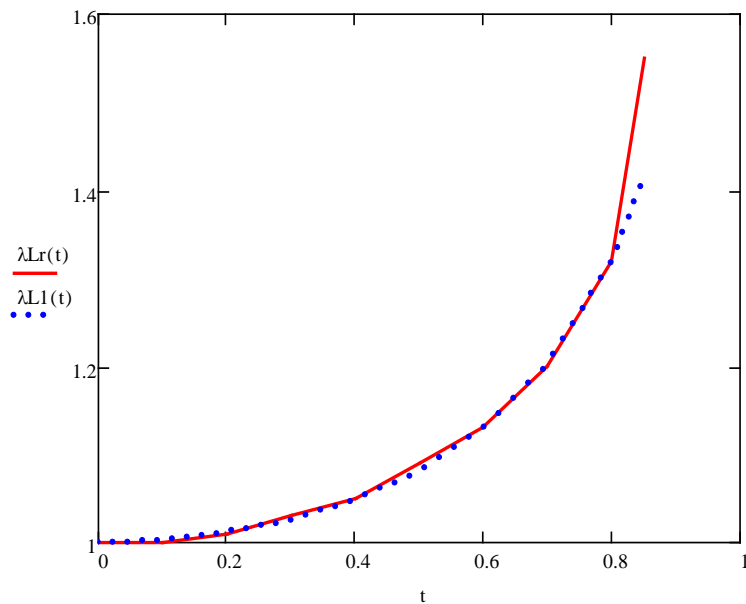

Figure 5. For Sample 5 in [1], the solid line is the plot of the reduced London penetration depth $\lambda_{Lr}(t) = \lambda_L(t)/\lambda_{L0}$ as obtained via theory in this paper. The overlapping plot is obtained via $\lambda_{L1}(t) = \left(1 - t^2\right)^{-0.27}$.

8) As concerns the rather accurate numerical fits that we have obtained for the values of various empirical parameters associated with j_c, it is remarkable that each of them is found to vary as some power of $(1 - t^2)$. Viewed in conjunction with (1), it provides another example of the deep physical insight that Bardeen had without the benefit of a detailed microscopic theory governing j_c.

5. Conclusions

It has been shown above that the GBCSEs-based approach provides a valuable alternative to the explanation of the Romijn *et al.*'s $j_c(T)$ empirical data for super-conducting Al strips based on the KL [3] approach derived from the Eilenberger equations which, in turn, follow from the microscopic Gor'kov theory when certain simplifying assumptions are made. Unique features of the GBCSEs-based approach are: 1) by appealing to the $j_c(0)$ value of an SC, it leads to a unique value of E_F that enables one to deal with its $\{\Delta, T_c, j_c(T)\}$ values in a unified framework, 2) with E_F thus fixed, appeal to the $j_c(t)$ values of the SC leads to a new finding about how $\gamma(t)$ varies with t, which is then shown to lead to (3 quantitative estimates of several T- and E_F-dependent superconducting parameters, viz., $s(t)$, $n_s(t)$, $v_c(t)$, $v_F(t)$, $\xi_r(t)$ and $\lambda_{Lr}(t)$. It is remarkable that one can obtain these results by remaining within the ambit of the mean-field approximation, *i.e.* by employing the model (constant) BCS interaction "$-V$", which for (6) in the scenario of 1PEM is operative only when $E_F - k\theta \le \left(\boldsymbol{P}/2 + \boldsymbol{p}\right)^2 \big/ 2m$, $\left(\boldsymbol{P}/2 - \boldsymbol{p}\right)^2 \big/ 2m \le E_F + k\theta$ and vanishes otherwise ([7], p. 117); for (2), (3) and (4), the corresponding constraints on V are obtained by putting $\boldsymbol{P} = 0$ in these inequalities and are identical with those in the usual BCS theory.

As was mentioned above, a plethora of formulae is known in the literature for calculating j_c of an SC, depending upon its type (I or II), size, shape and the manner of preparation. The application of E_F-incorporated GBCSEs herein, and to a variety of other SCs in [8] (with a correction in [10]), suggests that the E_F of an SC subsumes most of these properties.

We conclude by noting that work is in progress to further generalize the GBCSEs given here to deal with the pragmatic situation where the SC is in a heat bath in an external magnetic field, *i.e.* when both T and H are non-zero—a procedure for which has been given in [15].

Conflicts of Interest

The authors declare no conflicts of interest regarding the publication of this paper.

References

[1] Romijn, J., Klapwijk, T.M., Renne, M.J. and Mooij, J.E. (1982) Critical Pair-Breaking Current in Superconducting Aluminum Strips far below T_c. *Physical Review B*, **26**, 3648-3655. https://doi.org/10.1103/PhysRevB.26.3648

[2] Bardeen, J. (1962) Critical Fields and Currents in Superconductors. *Reviews of*

Modern Physics, **34**, 667-681. https://doi.org/10.1103/RevModPhys.34.667

[3] Kupriyanov, M.Y. and Lukichev, V.F. (1980) Temperature Dependence of Pair-Breaking Current in Superconductors. *Soviet Journal of Low Temperature Physics*, **6**, 210.

[4] Suhl, H., Matthias, B.T. and Walker, L.R. (1959) Bardeen-Cooper-Schrieffer Theory in the Case of Overlapping Bands. *Physical Review Letters*, **3**, 552-554. https://doi.org/10.1103/PhysRevLett.3.552

[5] McMillan, W.L. (1968) Transition Temperature of Strong-Coupled Superconductors. *Physical Review*, **167**, 331-344. https://doi.org/10.1103/PhysRev.167.331

[6] Malik, G.P. (2013) On a New Equation for Critical Current Density Directly in Terms of the BCS Interaction Parameter, Debye Temperature and the Fermi Energy of the Superconductor. *World Journal of Condensed Matter Physics*, **3**, 103-110. https://doi.org/10.4236/wjcmp.2013.32017

[7] Malik, G.P. (2016) Superconductivity: A New Approach Based on the Bethe-Salpeter Equation in the Mean-Field Approximation (Series on Directions in Condensed Matter Physics Book 21). World Scientific, Singapore. https://doi.org/10.1142/9868

[8] Malik, G.P. (2016) On the Role of Fermi Energy in Determining Properties of Superconductors: A Detailed Comparative Study of Two Elemental Superconductors (Sn and Pb), a Non-Cuprate (MgB_2) and Three Cuprates (YBCO, Bi-2212 and Tl-2212). *Journal of Superconductivity and Novel Magnetism*, **29**, 2755-2764. https://doi.org/10.1007/s10948-016-3637-5

[9] Malik, G.P. (2017) A Detailed Study of the Role of Fermi Energy in Determining Properties of Superconducting NbN. *Journal of Modern Physics*, **8**, 99-109. https://doi.org/10.4236/jmp.2017.81009

[10] Malik, G.P. (2018) Correction to: On the Role of Fermi Energy in Determining Properties of Superconductors: A Detailed Comparative Study of Two Elemental Superconductors (Sn and Pb), a Non-Cuprate (MgB_2) and Three Cuprates (YBCO, Bi-2212 and Tl-2212). *Journal of Superconductivity and Novel Magnetism*, **31**, 941-941. https://doi.org/10.1007/s10948-017-4520-8

[11] Poole, C.P. (2000) Handbook of Superconductivity. Academic Press, San Diego.

[12] Kresin, V.Z. and Zaĭtsev, G.O. (1978) Temperature Dependence of the Electron Specific Heat and Effective Mass. *Soviet Physics JETP*, **47**, 983.

[13] Kittel, C. (1974) Introduction to Solid State Physics. Wiley Eastern, New Delhi.

[14] Plumb, N.C., *et al.* (2009) Low-Energy (< 10 meV) Feature in the Nodal Electron Self-Energy and Strong Temperature Dependence of the Fermi Velocity in $Bi_2Sr_2CaCu_2O_{8+\delta}$ https://arxiv.org/pdf/0903.4900.pdf

[15] Malik, G.P. (2010) On Landau Quantization of Cooper Pairs in a Heat Bath. *Physica B*, **405**, 3475-3481. https://doi.org/10.1016/j.physb.2010.05.026